# J8.5 VERTICAL PROFILES OF CARBON DIOXIDE, TEMPERATURE, AND WATER VAPOR WITHIN AND ABOVE A SUBURBAN CANOPY LAYER IN WINTER

Ryo Moriwaki* and Manabu Kanda*
* Tokyo Institute of Technology, Tokyo, Japan

## 1. INTRODUCTION

Information on the vertical profile of scalar concentration within and above urban canopies is important for gaining an understanding of the scalar exchange process between cities and the atmosphere. Field experimental data on the vertical profile are also quite useful to evaluate modeling and wind tunnel experiments on the dispersion of scalars such as air pollutants within urban canopies (e.g., Briggs et al., 2001). Vogt et al. (2005) made urban field measurements for the vertical profile of $CO_2$ at a street canyon in Basel, Switzerland, and they reported that the profile was sensitive to the amount of local traffic and wind conditions. In addition, the turbulent transport process is generally sensitive to the dimensions of the surrounding building arrays (Kanda, 2005). Given that the vertical profiles are probably significantly different at different sites, it follows that urban field measurements should be done at a range of sites to fully understand the fluxes of $CO_2$ as well as the fluxes of other pollutants.

In this study we investigated the temporal change and the vertical profile of $CO_2$ within and above a residential canopy in Tokyo, Japan, on the basis of field measurements in winter. We also investigated those of air temperature and $H_2O$ concentration, which had different source locations..

## 2. METHODS

### 2.1 *Site Description*

A set of observations was done during November and December 2004 in a low-storied residential area in Kugahara, Tokyo, JAPAN (35º34'N, 139º41'E). A 29 m tower (without guy lines) was installed in the backyard of a home. The residential area consisted of houses with a mean height (zh) of 7.3 m, paved roads, and small playgrounds. The location of this site and a view from the tower is shown in Fig. 1. Flat, uniform terrain extends over 1 km to the south, west, and north from the tower. The terrain within 200 m to the east is gently slanting down with an inclination angle of 5.7o. About 33% of the area was buildings, 22% was vegetation, and 23% was impervious space such as paved roads and concrete. Additional details are given in Moriwaki and Kanda (2004). The tower is located 5 m away from a nearest building and 4 m away from an adjacent road. This road has almost no traffic. Therefore, the effect of traffic can be almost ignored especially for the observations within the canopy. In the vicinity of tower (within 50 m) a mean aspect ratio (building height to width of space) is 0.63.

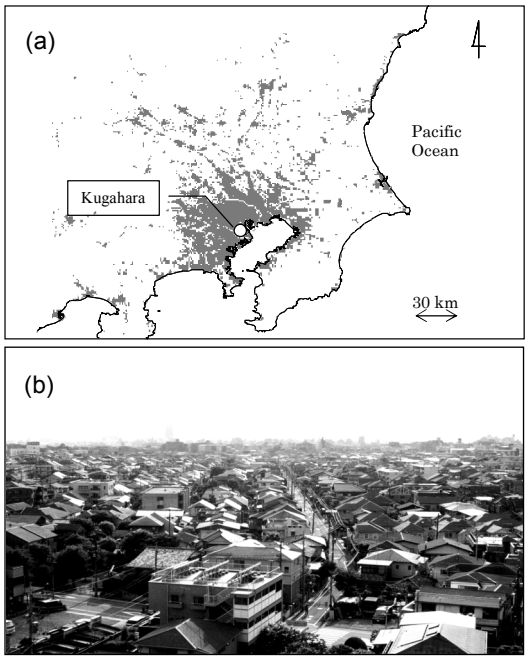


Fig. 1. (a) Location of Kugahara in Tokyo, Japan and (b) view to the west from the 20-m height of the tower. Gray area in Fig. (a) indicates built-up area where artificial structures occupy significant surfaces. The data source is "Global Map" (ISCGM: International Steering Committee for Global Mapping), available from http://www.iscgm.org/.

### 2.2 *Experimental Setup*

Sensible heat, latent heat, and $CO_2$ fluxes were measured at 29 m using a sonic anemometer (USA1, Metek GmbH) and an infrared $CO_2$/ $H_2O$ open-path analyzer (LI-7500, LI-COR). Other details of the tower and instrumental setting are in Fig. 2. This measurement height was found to be above the urban roughness layer according to our analysis of the flux-gradient relationships for momentum and heat (Moriwaki and Kanda, 2005). The instantaneous horizontal and vertical wind velocities $u$, $v$, and $w$, sonic temperature $T$, humidity $q$, and $CO_2$ concentration $c$, were sampled at 8 Hz. These data were logged to a data logger (CR10X, Campbell Sci.)

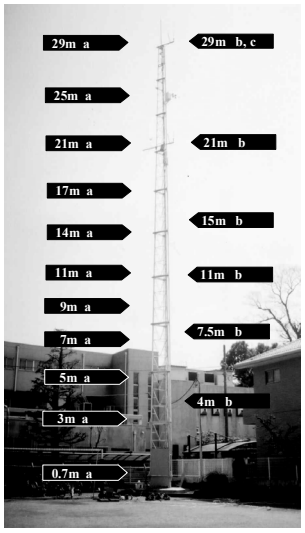


| | Variable |
|---|---|
| a | $CO_2$, $q$, $Ta$ |
| b | $u$, $v$, $w$, $Ts$ |
| c | $CO_2'$, $q'$ |

See text for the variables.

Fig. 2. View of the tower and instrumental setup.

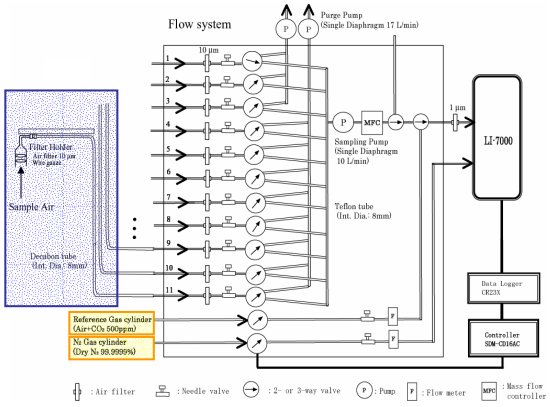


Fig. 3. Gas-multiplexer system for $CO_2$ and $H_2O$ concentrations.

and stored on a computer. Heat, water vapor, and $CO_2$ fluxes were estimated using the eddy-covariance method every 60 min. The coordinate axes were rotated so that the mean vertical and lateral vertical velocities were zero ( $\overline{v} = \overline{w} = 0$ ) and that the covariance $\overline{v'w'}$ was zero (McMillen, 1988), where the over-bar is temporal averaging and primes indicate fluctuation components. The water vapor and $CO_2$ fluxes were corrected for density effects (WPL correction; Webb et al. 1980). In addition to the measurements at 29 m, wind velocity and turbulent statistics were measured using sonic anemometers at 4, 7.5, 11, 15, and 21 m (Fig. 2) .

Air temperatures were measured using unshielded, 50-μm-thick bare thermocouples. Errors due to radiation on such fine gauge thermometers are within 0.1 K. The thermocouple signals were recorded every 1 second and averaged over 10 minutes. More details are in Kanda et al. (2005a).

The vertical profiles of $CO_2$ and vapor concentration were measured using a $CO_2/H_2O$ gas-multiplexer system sampled sequentially air from 11 tower levels. We located 11 levels with inlets for $CO_2/H_2O$-concentration measurements. Air was sucked from each inlet at the tower through a Decabon tube down into an air-conditioned room at the bottom of the tower, where a gas multiplexer and a LI7000 closed path gas-analyzer (LI-COR) were operated. To minimize the effect of temporal changes of the background concentration, we setup a quick switching system (Fig. 3) similar to the one reported by Xu et al. (1999) and Vogt et al. (2005). Air from different levels was continuously drawn through all the lines while air from one selected height was monitored in the LI-7000. Each channel was sampled for 10 seconds but the first 3 seconds after switching were discarded. Mean values over the remaining 7 seconds were stored. The measurements for all 11 levels took 2 minutes. The data in down-to-top switching order and that in top-to-down switching order were averaged together to cancel out the effect of temporal change of concentration in the atmosphere. These procedures resulted in a cycle of 4 minutes for the mean $CO_2/H_2O$ profiles at all 11 levels. The gas-analyzer was operated in differential mode, that is, by measuring continuously a zero gas in the reference cell. Every 60 minutes the standard gas for $CO_2$ (500 ppm) was supplied to the analyzer for 10 minutes for real time calibration. The intensive observation period was from November to December 2004.

### 2.3 *Data Processing*

To examine the stability effect on the mean profiles, we used the bulk Richardson number (*Rb*) which was determined based on data measured at 29 m and 3 m.

$$Rb \equiv \frac{gz}{T}\frac{\theta - \theta_s}{U^2} \quad , \qquad (1)$$

where $g$ is the acceleration due to gravity, $\theta$ is the potential temperature at 29 m, $\theta_s$ is given by the potential temperature at 3 m, $U$ is the wind speed at 29 m, and $T$ is the air temperature at 29 m. Virtual temperature is usually used, but here we assumed the virtual temperature to be approximately equal temperature. By definition, *Rb* represents the stability within and above the canopy, and thus it is the most suitable stability index for the vertical profile of $CO_2$ concentration. We set $Rb > 5$ for the stable case, and $Rb < -1$ for the unstable case. The number of datasets for stable and unstable cases is 17 and 26, respectively.

## 3. RESULTS AND DISCUSSION

The ensemble-averaged profiles of air temperature and $CO_2/H_2O$ concentrations for each case are shown in Fig. 4 along with the corresponding averages for the

wind speed and turbulent kinetic energy.

### 3.1 *Ensemble-Mean Profiles For Unstable Case*

**a) *Air temperature***

The data for the unstable case came mainly from daytime data. The air temperature profile (Fig. 4a) shows that the air temperature peaks near the rooftop level ($z/z_h$ = 1). Kanda et al. (2005a) investigated the seasonal trend of vertical temperature profiles and concluded that the height of the daily maximum temperature in this site is mainly dependent on the height at which solar energy is absorbed. In winter, more solar radiation is absorbed on the roofs and the upper part of the walls due to the lower solar angle in this season. Additional observations on the surface temperature using a thermal infrared camera showed that the roofs were the most-heated surfaces in the winter daytime (Fig. 5), which agree with the results of Hoyano et al. (1999). There is another peak near the ground level. This is attributed to the locality of the observation site. The dataset used for unstable case was from the morning, in which the solar heats not only roof but also the ground surface just around the tower. Therefore, in some of the dataset, the peak appeared at the lowest measurement level.

**b) $CO_2$ concentration**

The $CO_2$ concentration for the unstable case during daytime (Fig. 4b) is almost homogeneous within and above the canopy, although the $CO_2$ flux was upward even in the daytime (not shown here). Moriwaki and Kanda (2004) revealed that the major sources of $CO_2$ in this residential area are fossil fuel consumption in houses and traffic. However, limiting to the vicinity of tower, we can assume that the traffic is almost none. Therefore, the traffic can be ignored as a source of $CO_2$ within the canopy. Hereafter we only focus on the $CO_2$ emission from houses. Krüger et al. (1995) investigated the $CO_2$ concentration in four residential buildings and reported that indoor $CO_2$ concentration sometimes exceeded 1000 ppmv. The concentrated $CO_2$ is probably emitted through ventilating fans because the houses in this residential area do not have chimneys. The locations of the ventilating fans are usually in the middle or upper part of the canopy. Therefore, the emitted $CO_2$ from the houses were easily dispersed by larger turbulent mixing (Fig. 4e). The homogeneous $CO_2$ profile contrasts with the result reported by Vogt et al. (2005), who conducted field measurements in a street canyon. They found that the $CO_2$ concentration always decreased with height. The source of the anthropogenic $CO_2$ in Vogt et al. (2005) is mainly due to the traffic and is located on the street level where the turbulent intensity would be relatively small. In contrast, the location of the $CO_2$ emission in this study site is the middle or upper level within the canopy where the turbulent intensity is larger (Fig. 4e). Therefore, the emitted $CO_2$ was well-mixed and the resulting profile is homogeneous. The dispersion of $CO_2$ is also sensitive to the canopy geometry. Canyon

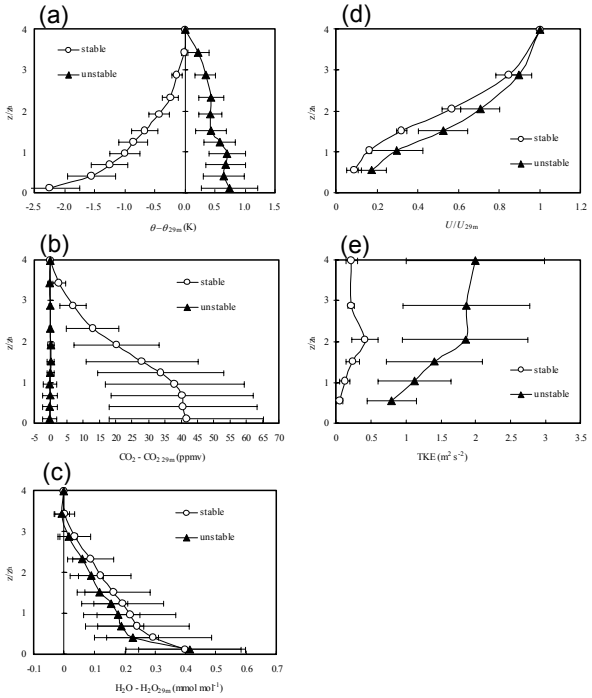


Fig. 4. Ensemble-mean profiles of (a) temperature, (b) $CO_2$ concentration, (c) $H_2O$ concentration, (d) wind speed normalized by $U_{4zh}$, and (e) turbulence kinetic energy (TKE) in stable and unstable case, respectively. Air temperature, $CO_2$, and $H_2O$ are the values subtracted from the values at z = 29 m.

height to ratio (H/W) is 1 in Vogt et al. (2005) while that in this study is 0.63 in the vicinity of the tower (within 50 m). The lower aspect ratio of this study indicates that the canopy is more dispersive and thus the scalar within the canopy is more easily diffused.

**c) $H_2O$ concentration**

On the other hand, the shape of the $H_2O$ profile for the unstable case (Fig. 4c) was quite different from that of $CO_2$. The $H_2O$ concentration was highest near the ground and there were differences within and above the canopy. This is probably because the emission of $H_2O$ was located in the vicinity of the ground surface (Moriwaki and Kanda, 2004). Daytime latent heat flux probably came mostly from the bare soil because most of the leaves on garden trees had fallen by early winter. The turbulent kinetic energy within the canopy is less than that above or in the upper part of the canopy (Fig. 4e), and thus the emitted $H_2O$ near the ground would not be well-mixed. This process is probably similar to the $CO_2$ profile of Vogt et al. (2005).

### 3.2 *Ensemble-Mean Profiles For Stable Case*

**a) *Air temperature***

Next, we turn our attention to the data for the stable case, which was mainly from the nighttime data. The air temperature profile (Fig. 4a) showed that the level with the minimum air temperature was located at

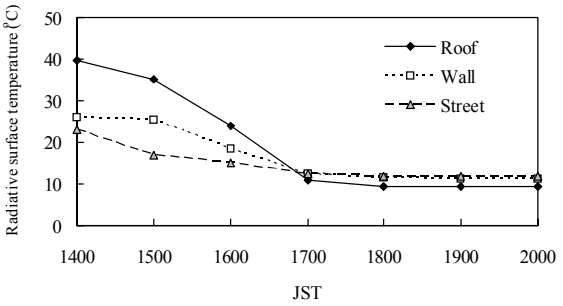


Fig. 5. Radiative surface temperature of roof, wall, and street measured using a thermal infrared camera from 1400 to 2000 JST on 15 February 2005.

the lowest measurement level ($z/z_h$ = 0.1). However, at night the roof has the lowest surface temperature in the canyon (Fig. 5). Usually, the roof is the surface that is more likely to be cooled during the nighttime because the large sky-view factor at the roof increases the radiative cooling there, compared with other surfaces within the canopy such as the wall and ground. The nighttime minimum surface temperature at the roof level was also reported for the city center of Marseille (Salmond et al., 2005) and for an outdoor scale model (Fig. 9 in Kanda et al., 2005b). The contrasting evidence between air temperature and surface temperature indicates that the cold air generated at roof level moved down to the ground level, causing the minimum of air temperature to occur at ground surface level. This is like a 'cold air pool' within the canopy and it would be possible under very calm and stably stratified conditions in which the wind speed and turbulent kinetic energy are low within the canopy (see Fig. 4d and 4e).

**b) $CO_2$ concentration**

The mean vertical profile of $CO_2$ for the stable case (Fig. 4b) shows that the $CO_2$ concentration within the canopy is much larger than that above the canopy, with a mean difference of 40 ppmv between the levels within and above the canopy. Interestingly, the $CO_2$ concentration above the roof top level decreases with height, while the $CO_2$ concentration within the canopy keeps almost the same level. The mean shape of the $CO_2$ vertical profile (Fig. 4b) indicates that the high flux of $CO_2$ emitted through the ventilating fans of houses (emitted from the upper part of the canopy) accumulates within the canopy. A possible reason for the dynamical behavior of $CO_2$ is the effect of 'cold air subsidence'. That is, the cold air that formed at roof level flowed down, brought concentrated $CO_2$ air parcels down towards ground, and fill up the air within the canopy with high $CO_2$.

**c) $H_2O$ concentration**

The profile of $H_2O$ for the stable case (Fig. 4c) shows that the height of $H_2O$ maximum appears at the lowest measurement level ($z/z_h$ = 0.1). The mechanism for this $H_2O$ profile in the stable case can be also attributed to the 'cold-air subsidence' as follows. Basically, the mixing ratio of $H_2O$ in the upper air is lower (e.g., Stull, 1988) and there is no significant source of $H_2O$ within the canopy except for the soils in the backyard (Moriwaki and Kanda, 2004). Therefore, for the case of $H_2O$, the subsidence flow from the roof level takes the less humid air downward and decreases the $H_2O$ concentration within the canopy except the region closest to the ground where the turbulent mixing is very weak and thus the scalar is hard to be diffused. As a result, the $H_2O$ concentration in the vicinity of the ground level is high and decreases rapidly next to the ground, and the profile of $H_2O$ is quite different from that of $CO_2$.

### 3.3 *Dynamics Of Scalar Profiles*

The relationships between the 'cold-air subsidence' and the scalar profiles are also visible in the height-temporal contour plot of scalar (Fig. 6). When the wind speed decreased at around 2005 JST (see black arrow in Fig. 6a), a high $CO_2$ concentration was detected at the rooftop level and the highly concentrated parcel did not disperse above the canopy, but rather approached the ground from 2005 to 2010 JST. When the high $CO_2$ concentration approached the ground from 2005 to 2010 JST (Fig. 6b), less $H_2O$ concentration around the rooftop level

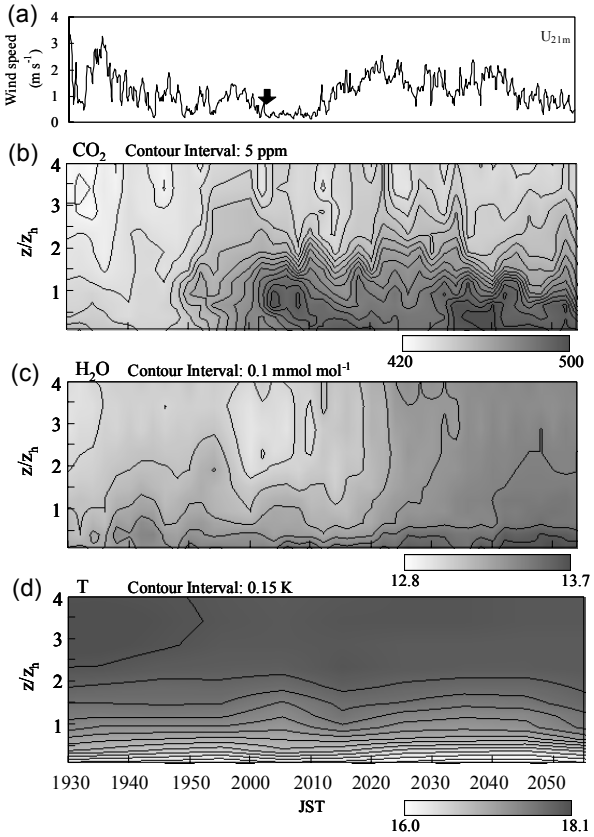


Fig. 6. One-half-hour time series of (a) horizontal wind speed measured at 21 m, (b) $CO_2$ concentrations, (c) $H_2O$ concentrations, and (d) air temperature from 1930 to 2100 JST on 15 December 2004.

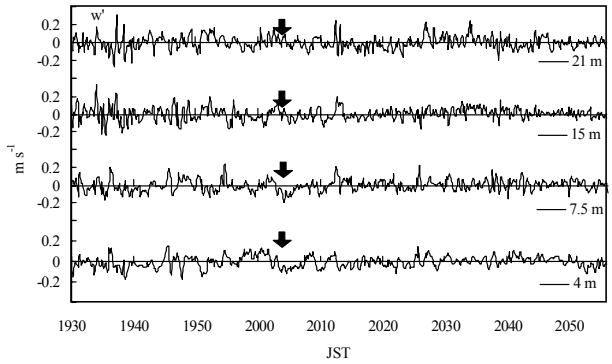


Fig. 7. One-half-hour time series of vertical wind velocity deviations measured at (a) 21 m, (b) 15 m, (c) 7.5 m, and (d) 4m from 1900 to 2100 JST on 15 December 2004.

was transferred downward into the canopy (Fig. 6c). Fig. 7 shows the vertical wind velocities at 21, 15, 7.5, and 4 m for the same time period of Fig. 6. Around 2005 JST, the vertical wind velocities within the canopy (both 4 and 7.5 m height) showed a slightly downward flow which is continuing for several minutes, although those above the canopy (15 and 21 m height) did not show any significant directed flows. The downward motion only within the canopy is consistent with the cold air subsidence that we described above.

## 4. CONCLUSIONS

We investigated the vertical profiles of air temperature, and $CO_2$/$H_2O$ concentration within and above a suburban surface layer.

The ensemble mean shape of the vertical profile for stably stratified conditions showed that the $CO_2$ emitted from the houses accumulated within the canopy. Such behavior was not found in the $H_2O$ profile. We argued that the reason for this difference is that a nocturnal cold-air subsidence flow brought down air parcels with high $CO_2$ concentrations from the ventilation fan to the ground. However, the largest $H_2O$ sources are at the ground, and thus the nocturnal cold-air flow did not bring $H_2O$ -rich air to the ground. As a result, $H_2O$ had a different vertical profile than $CO_2$ and instead decreased rapidly above the ground.

The present results and discussion indicate that urban micro-climate models should include both the three-dimensional turbulent flow around the building and the source distributions to accurately describe the dynamical behavior and diffusion processes of the scalars within and above urban canopies.

## ACKNOWLEDGEMENTS

This study was financially supported by CREST (Core Research for Evolution Science and Technology) of JST (Japan Science and Technology Agency) and by a Grant-in-Aid for Developmental Scientific Research from the Ministry of Education, Science and Culture of Japan. We thank Rev. Sister R. Kugimiya who kindly offered the land space for the field measurements.

## REFERENCES

Briggs, G.A., Britter, R.E., Hanna, S.R., Havens, J.A., Robins, A.G., Snyder, W.H., 2001. Dense gas vertical diffusion over rough surfaces: Results of wind-tunnel studies. Atmospheric Environment 35, 2265-2284.

Hoyano, A., Asano, K., Kanamaru, T., 1999. Analysis of the sensible heat flux from the exterior surface of buildings using time sequential thermography. Atmospheric Environment 33, 3941-3951.

Kanda, M., 2005. Large eddy simulations on the effects of surface geometry of building arrays on turbulent organized structures. Boundary-Layer Meteorology (in press)

Kanda, M., Moriwaki, R., Kimoto, Y., 2005a. Temperature profiles within and above an urban canopy. Boundary-Layer Meteorology 115, 499-506.

Kanda, M., Kawai, T., Kanega, M., Moriwaki, R., Narita, K-I., Hagishima, A., 2005b. Simple energy balance model for regular building arrays. Boundary-Layer Meteorology (in press)

Krüger, U., Kraenzmer, M., Strindehag, O., 1995. Field studies of the indoor air quality by photoacoustic spectroscopy. Environment International 21, 791-801.

McMillen, R.T., 1988. An eddy correlation technique with extended applicability to non-simple terrain. Boundary-Layer Meteorology 43, 231-245.

Moriwaki, R., Kanda, M., 2004. Seasonal and diurnal fluxes of radiation, heat, water vapor and $CO_2$ over a suburban area. Journal of Applied Meteorology 43, 1700-1710.

Moriwaki, R., Kanda, M., 2005. Flux-gradient profiles for momentum and heat over an urban surface. Theoretical and Applied Climatology, online first, DOI: 10.1007/s00704-005-0150-3.

Salmond, J.A., Oke, T.R., Grimmond, C.S.B, Roberts, S. M. Offerle, B., 2005. Venting of heat and carbon dioxide from street canyons at night. Journal of Applied Meteorology 44, 1180–1194.

Stull, R.B., 1988. An Introduction to Boundary Layer Meteorology. Kluwer Academic Publishers, pp. 670, Boston.

Vogt, R., Christen, A., Rotach, M.W., Roth, M., Satyanarayana, A.N.V., 2005. Temporal dynamics of $CO_2$ fluxes and profiles over a Central European city. Theoretical and Applied Climatology, online first, DOI: 10.1007/s00704-005-0149-9.

Webb, E.K., Pearman, G.I., Leuning, R., 1980. Correction of flux measurements for density effects due to heat and water vapour transfer. Quarterly Journal of Royal Meteorological Society 106, 85-100.

Xu, L.-K., Matista, A.A., Hsiao, T.C., 1999. A technique for measuring $CO_2$ and water vapor profiles within and above plant canopies over short periods. Agricultural and Forest Meteorology 94, 1-12.